SCIENTIFIC REPORTS

OPEN

SUBJECT AREAS:
CLIMATE-CHANGE IMPACTS
PHYSICAL OCEANOGRAPHY
ATMOSPHERIC DYNAMICS

Received
12 June 2014

Accepted
29 July 2014

Published
15 August 2014

Correspondence and requests for materials should be addressed to E.W. (wellerevan@postech.ac.kr)

More-frequent extreme northward shifts of eastern Indian Ocean tropical convergence under greenhouse warming

Evan Weller[1,2], Wenju Cai[1,3], Seung-Ki Min[2], Lixin Wu[3], Karumuri Ashok[4] & Toshio Yamagata[5]

[1]CSIRO Marine and Atmospheric Research, Aspendale, Victoria, Australia, [2]School of Environmental Science & Engineering, POSTECH, Pohang, Korea, [3]Physical Oceanography Laboratory, Qingdao Collaborative Innovation Center of Marine Science and Technology, Ocean University of China, Qingdao, China, [4]Centre for Climate Change Research, Indian Institute of Tropical Meteorology Pashan, Pune - 411 008, India, [5]Application Laboratory, JAMSTEC, 3173-25 Showa-machi, Kanazawa-ku, Yokohama 236-0001, Japan.

The Intertropical Convergence Zone (ITCZ) in the tropical eastern Indian Ocean exhibits strong interannual variability, often co-occurring with positive Indian Ocean Dipole (pIOD) events. During what we identify as an extreme ITCZ event, a drastic northward shift of atmospheric convection coincides with an anomalously strong north-minus-south sea surface temperature (SST) gradient over the eastern equatorial Indian Ocean. Such shifts lead to severe droughts over the maritime continent and surrounding islands but also devastating floods in southern parts of the Indian subcontinent. Understanding future changes of the ITCZ is therefore of major scientific and socioeconomic interest. Here we find a more-than-doubling in the frequency of extreme ITCZ events under greenhouse warming, estimated from climate models participating in the Coupled Model Intercomparison Project phase 5 that are able to simulate such events. The increase is due to a mean state change with an enhanced north-minus-south SST gradient and a weakened Walker Circulation, facilitating smaller perturbations to shift the ITCZ northwards.

The tropical eastern Indian Ocean is part of the Indo-Pacific warm pool, where the Earth's warmest SSTs support the rising branch of the Walker Circulation. In austral spring, westerlies flow over the northern equatorial Indian Ocean, which, together with the southeasterly trades south of the equator, feed convection near the warm pool (Fig. 1a), supplying the rising branch of the Walker Circulation[1–2]. The eastern Indian Ocean portion of the ITCZ is the locale of the most intense convective activity in the Indian Ocean basin[3]. Observed extreme ITCZ events in this region since 1979 tend to coincide with a pIOD or cooling off the Sumatra-Java coast[2–6]. However, the northward shift of the ITCZ is supported by a strong anomalous north-minus-south SST gradient in the eastern equatorial Indian Ocean[7] (Fig. 1b, c), and is accompanied by a large northward shift of the moisture convergence and precipitation axis by nearly 10 degrees latitude (~1000 km) from its climatological position during some of these events.

Given the strong rainfall gradient associated with the ITCZ, such an extreme shift leads to severe wild fires and drought for countries located directly within the climatological ITCZ position[2–3,8–13], but flooding in regions to the north, including Sri Lanka[8] in the southern parts of the Indian subcontinent. Other effects include widespread health problems to inhabitants of Indonesia and surrounding countries as a result of smoke and haze[2,13], and coral reef mortality across western Sumatra[14]. With such a dramatic impact on vulnerable nations, it is important to understand how extreme ITCZ events will change in a warmer climate. Here we show that greenhouse warming leads to a substantial increase in the frequency of extreme ITCZ events, and those future climate extremes can occur in the absence of concurrent pIOD events.

We identify a shift of the ITCZ using the location of the southern boundary of major tropical convection (greater than 3 mm day^{-1}) between 90°E–110°E, typically situated at ~10°S (Fig. 1a). In the three extreme ITCZ events over the observed satellite-era (2006, 1997, 1994), rainfall reduces dramatically in the equatorial southeastern Indian Ocean, and the ITCZ undergoes extreme shifts towards the equator by up to 1000 km (Fig. 1b–d). In contrast, when the ITCZ shifts southwards of its climatological position, rainfall increases only little (Fig. 1d). During 1997, rainfall over the equatorial southeastern Indian Ocean reduced to ~20% (~1.5 mm day^{-1}) of the seasonal mean and the ITCZ was confined to the Northern Hemisphere. The frequency is one event every ~11 years (3 events in 32 years).

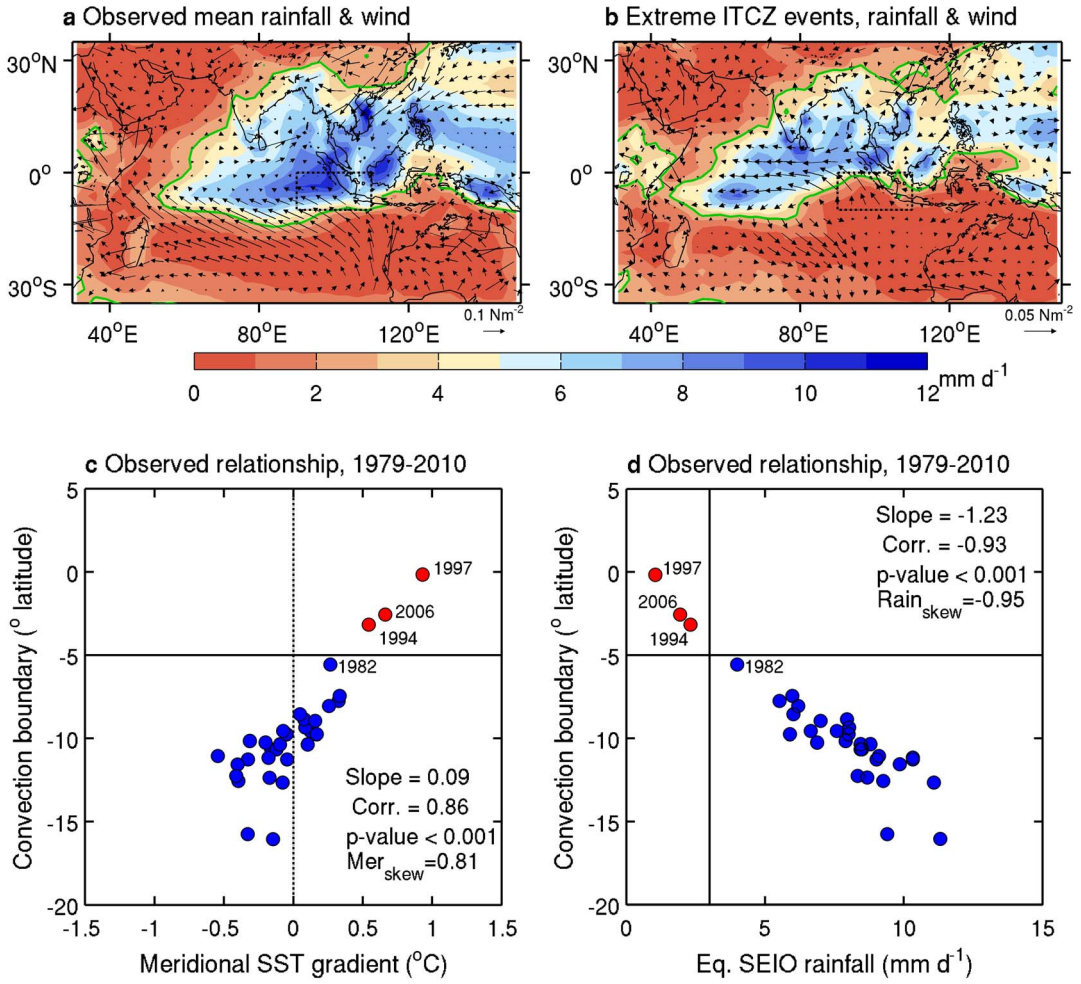

Figure 1 | Observed Indian Ocean austral spring conditions. (a), September to November (SON) mean rainfall from satellite-era data from the Global Precipitation Climatology Project Version 2[25] and reanalysis surface wind stress[27]. The 3 mm day^{-1} contour is indicated in green to highlight the boundary of the tropical convection. (b), Composite of SON mean rainfall and wind stress anomalies during extreme Indian Ocean tropical convergence zone (ITCZ) events. (c), Relationship between eastern equatorial Indian Ocean meridional (north-minus-south) SST[26] gradient (°C; 2.5°N–7.5°N, 90°E–110°E minus 10°S–5°S, 90°E–110°E) and the mean latitude of the southeastern Indian Ocean ITCZ boundary (between 90°E–110°E). Red dots highlight the identified extreme ITCZ events where the convection boundary shifts northward of 5°S (indicated by the solid horizontal line). (d), Relationship between the areal mean equatorial southeastern Indian Ocean (Eq. SEIO; 10°S–0°,90°E–110°E, dashed box in a, b) rainfall and the mean latitude of the southeastern Indian Ocean ITCZ boundary (between 90°E–110°E). This highlights that during extreme ITCZ events rainfall is dramatically reduced to less than 3 mm day^{-1} (indicated by the solid vertical line) in the southeastern Indian Ocean, i.e. the ITCZ climatological position. All maps were produced using licensed MATLAB.

Because the observed extreme ITCZ events are associated with a strong pIOD event, an equally significant relationship exists with the observed zonal (west-minus-east) SST gradient, as measured by the Dipole Mode Index (DMI[3]) over the equatorial Indian Ocean (Supplementary Fig. S1c, d). Therefore, an issue arises as to whether extreme ITCZ events are simply a characteristic of pIOD events (Supplementary Fig. S1b). Not all strong pIOD events are associated with an extreme shift of the ITCZ. For example, the 1982 pIOD event displayed a DMI of similar magnitude to the 1994 and 2006 events (Supplementary Fig. S1b), but there is no drastic shift of the ITCZ (Fig 1c, d). Thus an extreme ITCZ shift can be induced by the local north-minus-south SST gradient over the eastern equatorial Indian Ocean where the local dynamics are important. We show that in the future such an extreme shift can occur without a pIOD event, but with similar impacts.

Under greenhouse warming, SSTs are projected to warm faster in the west than off the Sumatra-Java coasts, facilitating reduced strength of the equatorial westerly winds and Walker Circulation during austral spring[15–18] (Supplementary Fig. S2a). However, in the eastern Indian Ocean, the north is also projected to warm faster than the south, due to its close proximity to a fast warming Asian landmass[19]. This translates to an increase in the mean north-minus-south SST gradient, facilitating an increase in northward cross-equatorial wind flow (Supplementary Fig. S2a). A future mean state with strengthened north-minus-south positive SST gradients and a weakened Walker Circulation (referenced to the present-day)[19] (Supplementary Fig. S2a) can be favourable for extreme ITCZ events.

To assess the influence of greenhouse warming, the Historical simulation and the Representative Concentration Pathways 8.5 (RCP 8.5) experiment from the Coupled Model Intercomparison Project phase 5 (CMIP5[20]) multi-model database are used to represent the present and future climates. Not all of the 25 coupled general circulation models (CGCMs) considered here are able to simulate the characteristics of the observed mean state of the tropical Indian Ocean and interannual variability[17,21–22] (i.e. the IOD). We examine the 13 CGCMs that simulate negative skewness of rainfall over the equatorial southeastern Indian Ocean, a criterion needed to capture those models that display a realistic rainfall mean state in the ITCZ

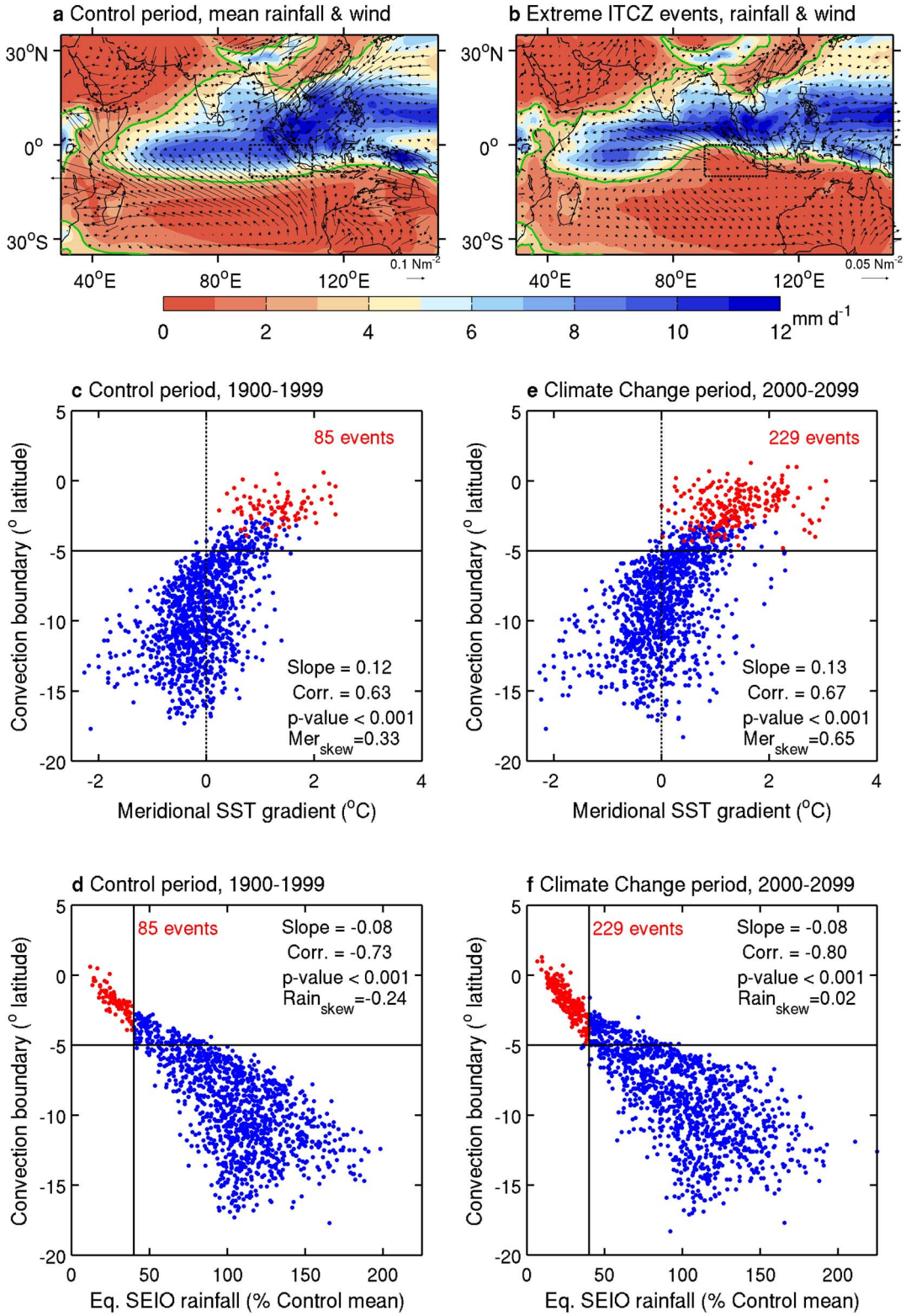

Figure 2 | Multi-model ensemble of the Indian Ocean austral spring conditions. (a), September to November (SON) mean rainfall and surface wind stress during the Control period (1900–1999). The 3 mm day^{-1} contour is indicated in **green** to highlight the position of the boundary of the tropical convection. (b), Composite of SON mean rainfall and wind stress anomalies during extreme Indian Ocean tropical convergence zone (ITCZ) events. (c), Relationship between eastern equatorial Indian Ocean meridional (north-minus-south) SST gradient (°C; 2.5°N–7.5°N, 90°E–110°E minus 10°S–5°S, 90°E–110°E) and the mean latitude of the southeastern Indian Ocean ITCZ boundary (between 90°E–110°E) for the Control period (1900–1999). (d), Relationship between the areal mean equatorial southeastern Indian Ocean (Eq. SEIO; 10°S–0°,90°E–110°E, dashed box in (a), (b)) rainfall and the mean latitude of the southeastern Indian Ocean ITCZ boundary (between 90°E–110°E) for the Control period (1900-1999). In (c) and (d), red dots highlight the identified extreme ITCZ events where the convection boundary shifts north of 5°S (indicated by the solid horizontal line) and rainfall is dramatically reduced to less than 40% of the Control period mean (indicated by the solid vertical line) in the equatorial southeastern Indian Ocean. (e), (f), The same as (c) and (d) but for the Climate Change period (2000–2099). All maps were produced using licensed MATLAB.

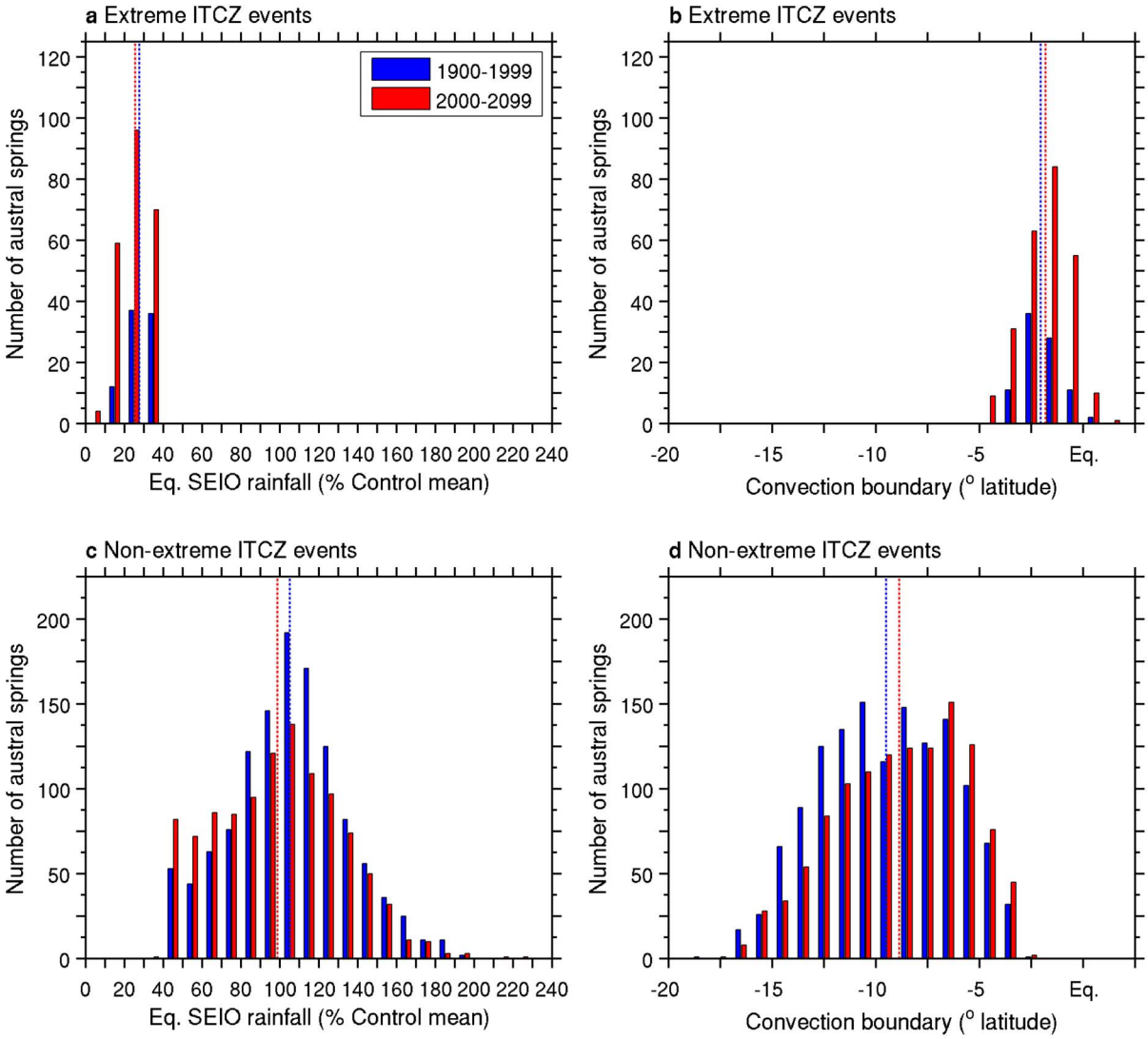

Figure 3 | Multi-model statistics associated with the increase in frequency of extreme Indian Ocean tropical convergence zone (ITCZ) events in austral spring. (a), Multi-model ensemble histogram of areal mean equatorial southeastern Indian Ocean (Eq. SEIO; 10°S–0°, 90°E–110°E) rainfall (percentage referenced to the Control period mean) during extreme ITCZ events. Values during extreme ITCZ years in each period are separated in 10% bins centred between the tick point for the Control (blue) and Climate Change (red) period. The multi-model median for the Control (dashed blue line) and the Climate Change (dashed red line) periods are indicated. (b), The same as a but for the boundary of the ITCZ over the southeastern Indian Ocean (between 90°E–110°E) (separated in 1° latitude bins). (c), (d), The same as (a), (b) but for all years excluding extreme ITCZ events. In the extreme ITCZ panels, the two histograms are not statistically different, but are in the non-extreme ITCZ panels and in each period for extreme ITCZ and non-extreme ITCZ, above the 95% confidence level.

(Fig. 2a). Using this selection also captures CGCMs that simulate the non-linearity associated with the interannual variability, observed in the tropical eastern Indian Ocean north-minus-south SST gradient (positive gradients exhibiting larger amplitudes than negative) and equatorial southeastern Indian Ocean rainfall anomalies (Supplementary Table 1). We compare the frequency in the first (1900–1999) and second (2000–2099) 100-year periods, referred to as the Control and Climate Change periods, respectively.

Despite a distinct bias in the CGCMs where the ITCZ extends too far to the west (comparing Fig. 2a to Fig. 1a), the selected CGCMs display the same relationships in the tropical eastern Indian Ocean as is observed (Fig. 2b–d). There are significant connections between the tropical eastern Indian Ocean north-minus-south SST gradient, equatorial southeastern Indian Ocean rainfall and extreme shifts of the ITCZ towards the equator during the Control period.

We classify extreme ITCZ events as for the observed. To normalise across the CGCMs (due to the fact they have differing mean states), we use a threshold of 40% of the Control period seasonal mean equatorial southeastern Indian Ocean rainfall, equivalent to the 3 mm day^{-1} threshold and a mean state of 7.5 mm day^{-1} (i.e. 40%) in the observed (Fig. 1d) during austral spring. The location of the ITCZ boundary in the selected multi-model ensemble is realistic (comparing Fig. 2a to 1a); therefore we similarly use 5°S as the threshold to define an extreme northward shift of the ITCZ towards the equator.

The frequency of extreme ITCZ events based on these definitions increases by approximately 170%, from about one event every ~15 years (85 events in 1300 years) in the Control period, to one every ~6 years (229 events in 1300 years) in the Climate Change period (Fig. 2c–f). This is statistically significant according to a bootstrap test[23], supported by a strong inter-model consensus, with 10 out of 13 models (77%) simulating an increase, and is confirmed by sensitivity tests to varying definitions of extreme ITCZ events (Supplementary Table 2). In both the Control and Climate Change periods, extreme

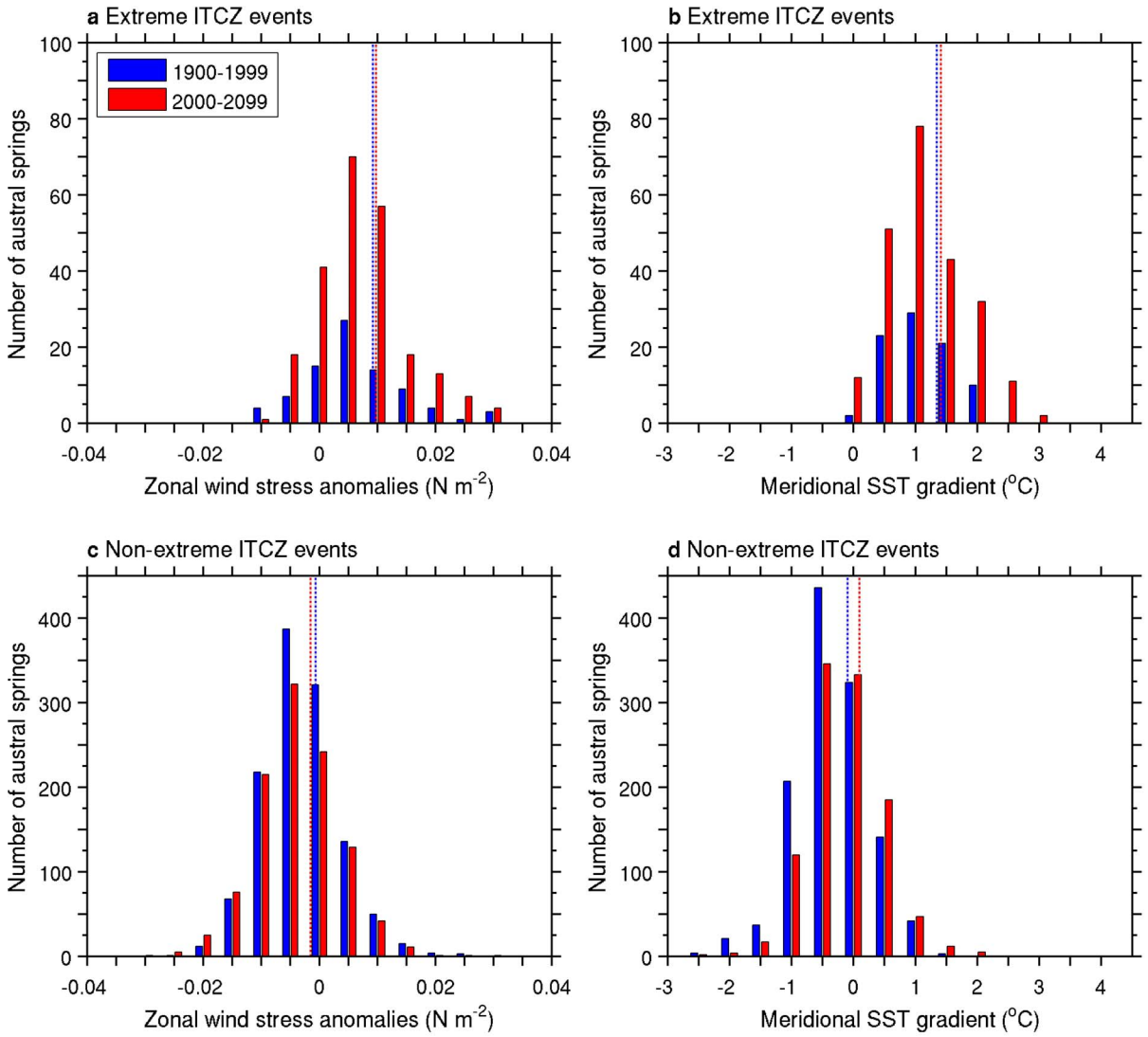

Figure 4 | Multi-model statistics associated with the increase in frequency of extreme Indian Ocean tropical convergence zone (ITCZ) events in austral spring. (a), Multi-model ensemble histogram of equatorial Pacific (5°S–5°N, 120°E–250°E) zonal wind stress anomalies during extreme ITCZ events. Values during extreme ITCZ years in each period are separated in 0.005N m^{-2} bins centred between the tick point for the Control (blue) and Climate Change (red) period. The multi-model median for the Control (dashed blue line) and the Climate Change (dashed red line) periods are indicated. (b), The same as a but for the eastern equatorial Indian Ocean meridional (north-minus-south) SST gradient (2.5°N–7.5°N, 90°E–110°E minus 10°S–5°S, 90°E–110°E) (separated in 0.5°C bins). (c), (d), The same as (a), (b) but for all years excluding extreme ITCZ events. The two histograms are statistically different in panel (d) only, and in each period for extreme ITCZ and non-extreme ITCZ, above the 95% confidence level.

ITCZ events are synchronised with a strong positive north-minus-south SST gradient over the eastern equatorial Indian Ocean, contraction of the warm pool, and associated convection to the north.

In the Climate Change period, approximately 46% of the extreme ITCZ events occur with a concurrent pIOD event (Supplementary Fig. S3 and Supplementary Table 3). By contrast, almost all extreme ITCZ events in the Control period occur with a pIOD event. The increasing frequency in extreme ITCZ events is not due to an increased frequency of pIOD events. In fact, there is little change in either the overall frequency (Supplementary Fig. S3 and Supplementary Table 3) or amplitude of pIOD events, defined using SST anomalies referenced to the evolving mean state[19].

Instead, the increased occurrences in the extreme ITCZ events are generated because of a gradual increase in the mean eastern equatorial Indian Ocean north-minus-south SST gradients (Supplementary Fig. 2b), referencing to a fixed-period mean climate. Because of the gradual increase in the SST gradient, it takes a smaller anomaly in the future climate to generate maximum SST to the north, facilitating more occurrences of reduced rainfall in the equatorial southeastern Indian Ocean and an increased frequency of extreme ITCZ events. As illustrated in Fig. 3, for a given size of rainfall reduction or a given convection boundary, there are more occurrences of extreme ITCZ events (Fig. 3a, b).

The increased frequency in extreme ITCZ events is not simply arising from a reduction in mean rainfall over this region, or a mean shift in the ITCZ, as evidenced by the differing patterns between the two periods (Supplementary Fig. S4). The different pattern also suggests that the mean state change is realised through non-extreme ITCZ events.

The increase in extreme ITCZ events under greenhouse warming is consistent with a weakening of the Walker Circulation[15–18] (Supplementary Fig. S5a). On interannual time scales, a weaker Walker Circulation tends to be associated with a northward shift of the ITCZ (Supplementary Fig. S5b). Comparing composites for extreme ITCZ events between the Control and Climate Change period, there is no significant change in the equatorial Pacific zonal wind

stress anomalies or the north-minus-south SST gradient anomalies during extreme ITCZ events between the Control and Climate Change period (Fig. 4a, b), despite the weakening Walker Circulation. This suggests that the impacts of extreme ITCZ events in the future are not more severe, but the number of occurrences increases. For a given wind stress anomaly (Fig. 4a), or a given strength of the eastern equatorial Indian Ocean north-minus-south SST gradient (Fig. 4b), there are increased occurrences of extreme ITCZ events.

The increased occurrences of extreme ITCZ events are not caused by an increased frequency of extreme pIOD events defined using rainfall, featuring high rainfall in the equatorial western Indian Ocean and enhanced subsidence along the equator[24]. The difference in equatorial zonal SST gradient between extreme ITCZ events of the two periods is significant (Supplementary Fig. S6), and would be more favourable for extreme pIOD events. However, only 40% in the Control and 55% in the Climate Change period of the extreme ITCZ events occur concurrently with such an extreme pIOD (Supplementary Fig. S7). This is again not surprising, because an extreme ITCZ event is governed by a north-minus-south SST gradient over the eastern Indian Ocean, while an extreme pIOD event is governed by anomalous advection of west-minus-east SST gradient[24].

In summary, increased occurrences of extreme northward shifts of the Indian Ocean ITCZ is consistent with the background state changes under greenhouse warming. Other factors, such as sub-seasonal tropical phenomena like the Madden-Julian Oscillation, may also contribute to an increased variability in the Indian Ocean ITCZ, particularly in other seasons. Here we emphasise the role of mean state change in austral spring. With the projected large percentage increase, we expect more frequent occurrences of events such as droughts and bushfires for the maritime continent and surrounding islands, and also floods in other regions, such as southern parts of the Indian subcontinent, conditions generally experienced during present-day pIOD events. These will no longer be rare occurrences, but common for the regions that are affected by the ITCZ, regardless of future changes in pIOD events.

Methods

Diagnosis of observed extreme ITCZ events. Extreme ITCZ events were diagnosed using a suite of distinctive process-based indicators, such as low rainfall and retreat of the Indian Ocean tropical convergence zone (ITCZ) towards the equator over the tropical eastern Indian Ocean. This is associated with a north-minus-south SST gradient over the eastern equatorial Indian Ocean[7], defined as the difference of the areal mean SST anomalies in the northeastern Indian Ocean (2.5°N–7.5°N, 90°E–110°E) and southeastern Indian Ocean (10°S–5°S, 90°E–110°E) regions. We also employ the traditional DMI[3], defined as the difference of the areal mean SST anomalies in the western Indian Ocean (IODW; 10°S–10°N, 50°E–70°E) and eastern Indian Ocean (IODE; 10°S–0°, 90°E–110°E) regions. For observations, we focus on historical events in the satellite era (1979–present) using Global Precipitation Climatology Project Version 2 monthly precipitation analysis[25], SSTs[26] and wind stress from global reanalysis[27]. We focus on austral spring, September–November (SON), in which extreme shifts of the ITCZ occur and a pIOD typically peaks.

Analysis and selection of models. Under greenhouse warming, CGCMs suggest that the temperature difference between the two Indian Ocean regions involved in the north-minus-south and zonal dipole will increase and the mean condition will resemble what is now the positive state of the IOD (Supplementary Fig. S2). Therefore the eastern equatorial Indian Ocean north-minus-south SST gradient or traditional DMI are not sufficient to differentiate an ITCZ event as we need to change our definition to refer to future mean conditions. Thus, we propose an identification method in which we define an extreme ITCZ event as when the equatorial southeastern Indian Ocean rainfall is less than 40% of the Control period (1900–1999) mean, and the boundary of the ITCZ over the eastern Indian Ocean (between 90°E–110°E) shifts north of 5°S. This definition exclusively captures the three strongest observed ITCZ (and pIOD events as determined by the DMI) that experienced the largest northward shift of the ITCZ. To select CGCMs, the method is applied to 25 CMIP5 CGCMs, each covering 105 years of a pre-21st century climate change simulation using historical anthropogenic and natural forcings (1901-2005) and a further 95 years (2006–2100) under the RCP8.5 forcing scenario[20]. We compare the change in frequency of events between two periods, the Control period (1900–1999) to Climate Change period (2000–2099).

The mean state rainfall of some CGCMs is rather unrealistic in the Indian Ocean tropical convergence zone, simulating much drier conditions compared to observations during austral spring, which is ~7.5 mm day^{-1} since 1979. Related to the mean state, although the majority of CGCMs generate IOD-like variability, only a subgroup of CGCMs simulate the observed nonlinear ocean-atmosphere coupling over the eastern Indian Ocean as depicted by the negative skewness of rainfall anomalies during the austral spring, which is −0.95 in observations since 1979. The level of nonlinearity varies vastly among CGCMs, and we consider negative skewness of any extent. Out of the 25 CGCMs, 13 satisfy the rainfall skewness criterion. The selected CGCMs yield a mean skewness of −0.55 and a mean rainfall of 7.2 mm day^{-1}, close to the observed.

Statistical significance test. We use a bootstrap method[23] to test whether the change in frequency of the extreme ITCZ events is statistically significant. The 1,300 samples from the 13 selected CMIP5 CGCMs in the Control period are re-sampled randomly to construct another 10,000 realisations of 1,300-year records. In the random re-sampling process, any one extreme ITCZ event is allowed to be selected again. The standard deviation of the extreme ITCZ frequency in the inter-realisation is 8.9 events per 1,300 years, far smaller than the difference of 144 events per 1,300 years between the Control and the Climate Change periods (Fig. 2c, e), indicating a strong statistical significance. The maximum frequency is 121, far smaller than that in the Climate Change period of 229. Increasing the realisations to 20,000 or 30,000 yields similar results.

We also employ a Student's t-test to delineate significant regions of change (Climate Change minus Control) in the results reported; with a 95% confidence level (P-value < 0.05).

1. Neale, R. & Slingo, J. The maritime continent and its role in the global climate. *J. Clim.* **16**, 834–848 (2003).
2. Schott, F. A., Xie, S.-P. & McCreary, J. P. Indian Ocean circulation and climate variability. *Rev. Geophys.* **47**, RG1002, doi:10.1029/2007RG000245 (2009).
3. Saji, N. H., Goswami, B. N., Vinayachandran, P. N. & Yamagata, T. A dipole in the tropical Indian Ocean. *Nature* **401**, 360–363 (1999).
4. Webster, P. J., Moore, A. M., Loschnigg, J. P. & Leben, R. R. Coupled oceanic-atmospheric dynamics in the Indian Ocean during 1997–98. *Nature* **401**, 356–360 (1999).
5. Yu, L. & Rienecker, M. M. Mechanisms for the Indian Ocean warming during the 1997–98 El Niño. *Geophys. Res. Lett.* **26**, 735–738 (1999).
6. Murtugudde, R., McCreary, J. P. & Busalacchi, A. J. Oceanic processes associated with anomalous events in the Indian Ocean with relevance to 1997–1998. *J. Geophys. Res.* **105**, 3295–3306 (2000).
7. Weller, E. & Cai, W. Meridional variability of atmospheric convection associated with the Indian Ocean Dipole Mode. *Sci. Rep.* **4**, 3590 DOI:10.1038/srep03590 (2014).
8. Zubair, L., Rao, S. A. & Yamagata, T. Modulation of Sri Lankan Maha rainfall by the Indian Ocean dipole. *Geophys. Res. Lett.* **30**, 1063, doi:10.1029/2002GL015639 (2003).
9. Meyers, G. A., McIntosh, P. C., Pigot, L. & Pook, M. J. The years of El Niño, La Niña, and interactions with the tropical Indian Ocean. *J. Clim.* **20**, 2872–2880 (2007).
10. Ummenhofer, C. C. *et al.* What causes southeast Australia's worst droughts? *Geophys. Res. Lett.* **36**, L04706, doi:10.1029/2008GL036801 (2009).
11. Ashok, K., Guan, Z. & Yamagata, T. Influence of the Indian Ocean Dipole on the Australian winter rainfall. *Geophys. Res. Lett.* **30**, L1821, doi:10.1029/2003GL017926 (2003).
12. Cai, W., Cowan, T. & Raupach, M. Positive Indian Ocean Dipole events precondition southeast Australia bushfires. *Geophy. Res. Lett.* **36**, L19710, doi:10.1029/2009GL039902 (2009).
13. Page, S. E., Siegert, F., Rieley, J. O., Boehm, H.-D. V., Jaya, A. & Limin, S. The amount of carbon released from peat and forest fires in Indonesia in 1997. *Nature* **420**, 61–65 (2002).
14. Abram, N. J., Gagan, M. K., McCulloch, M. T., Chappell, J. & Hantoro, W. S. Coral reef death during the 1997 Indian Ocean Dipole linked to Indonesian wildfires. *Science* **301**, 952–955 (2003).
15. Vecchi, G. A. & Soden, B. J. Global warming and the weakening of the tropical circulation. *J. Clim.* **20**, 4316–4340 (2007).
16. Xie, S.-P. *et al* Global warming pattern formation: sea surface temperature and rainfall. *J. Clim.* **23**, 966–986 (2010).
17. Zheng, X. T. *et al.* Indian Ocean Dipole response to global warming in the CMIP5 multi-model ensemble. *J. Clim.* **26**, 6067–6080 (2013).
18. Huang, P., Xie, S.-P., Hu, K., Huang, G. & Huang, R. Patterns of the seasonal response of tropical rainfall to global warming. *Nature Geosci.* **6**, 357–361 (2013).
19. Cai, W. *et al.* Projected response of the Indian Ocean Dipole to greenhouse warming. *Nature Geosci.* **6**, 999–1007 (2013).
20. Taylor, K. E., Stouffer, R. J. & Meehl, G. A. An overview of CMIP5 and the experimental design. *Bull. Amer. Met. Soc.* **93**, 485–498 (2012).
21. Liu, L. *et al.* Indian Ocean variability in the CMIP5 multi-model ensemble: the zonal dipole mode. *Clim. Dyn.* 10.1007/s00382-013-2000-9 (2014).
22. Chu, J.-E. *et al.* Future change of the Indian Ocean basin-mode and dipole modes in the CMIP5. *Clim. Dyn.* **43**, 535–551, 10.1007/s00382-013-2002-7 (2014).

23. Austin, P. C. Bootstrap Methods for Developing Predictive Models. *The American Statistician* **58**, 131–137 (2004).
24. Cai, W. *et al.* Increased frequency of extreme Indian Ocean Dipole events due to greenhouse warming. *Nature* **510**, 254–258 (2014).
25. Adler, R. F. *et al.* The Version 2 Global Precipitation Climatology Project (GPCP) Monthly Precipitation Analysis (1979-Present). *J. Hydrometeor.* **4**, 1147–1167 (2003).
26. Rayner, N. A. *et al.* Global analyses of sea surface temperature, sea ice, and night marine air temperature since the late nineteenth century. *J. Geophys. Res.* **108**, 4407 (2003).
27. Kalnay, E. *et al* The NCEP/NCAR 40-Year Reanalysis Project. *Bull. Amer. Meteor. Soc.* **3**, 437–471 (1996).

Acknowledgments

This research is partly supported by the Australian Climate Change Science Program, and the Goyder Institute. W.C. is also supported by a CSIRO Office of Chief Executive Science Leader award. S.-K. M. was supported by the Korea Meteorological Administration Research and Development Program under Grant CATER 2013-3180.

Author contributions

E.W. and W.C. conceived the study. E.W. performed the model output analysis and wrote the initial draft of the paper. E.W., W.C., S-K.M., L.W., K.A. and T.Y. contributed to interpreting results, discussion of the associated dynamics, and improvement of this paper.

Additional information

Supplementary information accompanies this paper at http://www.nature.com/scientificreports

Competing financial interests: The authors declare no competing financial interests.

How to cite this article: Weller, E. *et al.* More-frequent extreme northward shifts of eastern Indian Ocean tropical convergence under greenhouse warming. *Sci. Rep.* **4**, 6087; DOI:10.1038/srep06087 (2014).